

Label-Free Fiber-Optic Raman Spectroscopy for Intravascular Coronary Atherosclerosis and Plaque Detection

Hao Jia, Xun Chen,* Jiahao Shen, Rujia Liu, Peipei Hou,* and Shuhua Yue*



Cite This: *ACS Omega* 2024, 9, 27789–27797



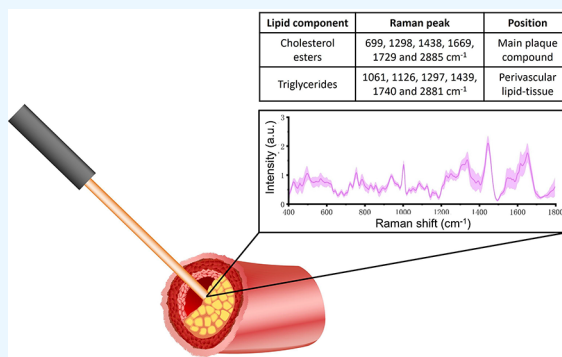
Read Online

ACCESS |

Metrics & More

Article Recommendations

ABSTRACT: The rupture of atherosclerotic plaques remains one of the leading causes of morbidity and mortality worldwide. The plaques have certain pathological characteristics including a fibrous cap, inflammation, and extensive lipid deposition in a lipid core. Various invasive and noninvasive imaging techniques can interrogate structural aspects of atheroma; however, the composition of the lipid core in coronary atherosclerosis and plaques cannot be accurately detected. Fiber-optic Raman spectroscopy has the capability of in vivo rapid and accurate biomarker detection as an emerging omics technology. Previous studies demonstrated that an intravascular Raman spectroscopic technique may assess and manage the therapeutic and medication strategies intraoperatively. The Raman spectral information identified plaque depositions consisting of lipids, triglycerides, and cholesterol esters as the major components by comparing normal region and early plaque formation region with histology. By focusing on the composition of plaques, we could identify the subgroups of plaques accurately and rapidly by Raman spectroscopy. Collectively, this fiber-optic Raman spectroscopy opens up new opportunities for coronary atherosclerosis and plaque detection, which would assist optimal surgical strategy and instant postoperative decision-making. In this paper, we will review the advancement of label-free fiber-optic Raman probe spectroscopy and its applications of coronary atherosclerosis and atherosclerotic plaque detection.



INTRODUCTION

The natural history of atherosclerotic coronary artery disease is general progression, which may be complicated by a variety of adverse events such as plaque rupture or erosion.^{1,2} When the plaque begins to encroach on the lumen, the coronary arteries will produce evident stenosis. Therefore, identifying the luminal diameter and plaque progression is critical for the detection of coronary atherosclerosis. Over recent years, there have been improvements in coronary imaging modalities that can assess plaque volumes using noninvasive techniques, such as intravascular ultrasound (IVUS) and optical coherence tomography (OCT).^{3–5} Both IVUS and OCT make use of an intracoronary imaging modality to deliver cross-sectional images of plaque morphologies, which can be indicative for certain plaque types. One of the most prominent features of IVUS is visibility of the full thickness of the vessel wall, usually reaching a penetration depth of several millimeters.^{6,7} In particular, the researchers recently reported an all-optical IVUS (AO-IVUS) imaging system, presenting 18.6 μm axial resolution, 124 μm lateral resolution, and 7 mm imaging depth, to depict details in vascular structures.⁸ Conversely, OCT demonstrates higher resolution than that of IVUS at about 2–10 μm but does not penetrate the plaque far enough to provide information about deep morphology.⁹ To improve diagnostic accuracy for atherosclerotic plaques, IVUS-OCT

integrated imaging devices have been developed that can have multiple functions in a single catheter and combine the superior features of each technology.^{10,11}

Anatomically, studies indicated that the development of atherosclerotic plaques is accompanied by complicated alteration of different components, including extensive lipid deposition, accumulation of cholesterol crystals, formation of fibrous cap collagen, inflammation, and so on.^{12–14} Such dramatic compositional heterogeneity highlights an urgent need to develop novel analytical methods with chemical selectivity to improve the efficiency of atherosclerotic plaque detection. To address this problem, intravascular spectroscopy techniques have been developed to provide additional compositional information about plaque pathobiology to address the limitations of both IVUS and OCT. For example, with the injection of specific imaging agents, near-infrared fluorescence imaging has been developed to not only map the

Received: February 19, 2024

Revised: May 15, 2024

Accepted: June 12, 2024

Published: June 20, 2024



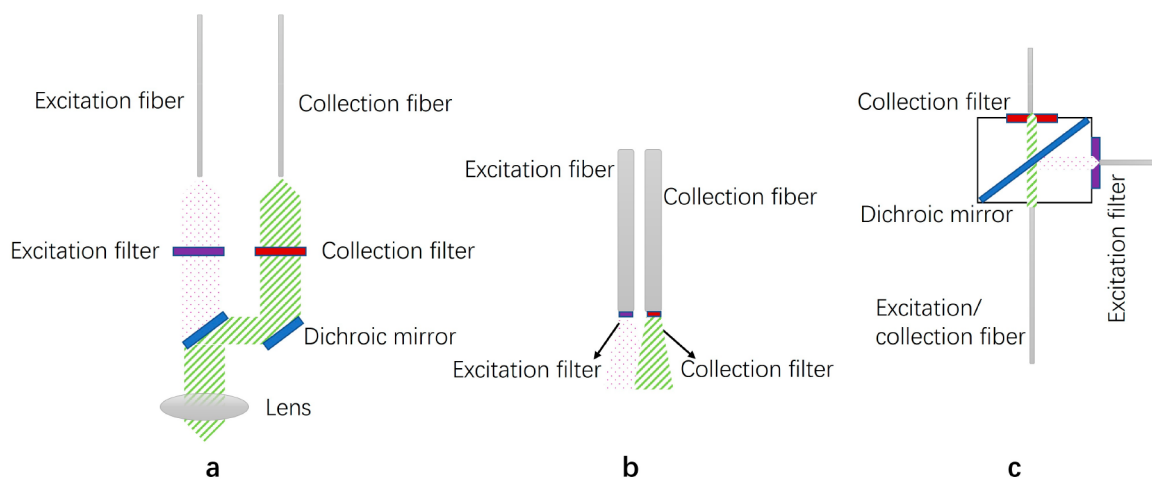


Figure 1. Three ways to realize Raman probes. (a) The principle of proximal filters from tissue sample. (b) The principle of coating multimode excitation and collection fibers. (c) The principle of remote filters from a tissue sample. The excitation filters, collection filters, and dichroic mirrors were represented in magenta color, red color, and blue color, respectively.

arterial inflammation¹⁵ but also provide lipid information on coronary plaques.¹⁶ In addition, intravascular spectroscopy with the use of fluorescence lifetime imaging provides valuable information for characterizing atherosclerotic lesions in coronary arteries, including the superficial presence of macrophage foam cells and extracellular lipid content in advanced lesions.¹⁷

As an alternative, vibrational spectroscopy, including Raman and near-infrared spectroscopy (NIRS), can interpret the chemical structure of biological samples with a noninvasive manner.¹⁸ Studies have demonstrated that NIRS is able to characterize low-density lipoprotein cholesterol accumulation^{19,20} and identify lipid core-containing plaques²¹ in patients with coronary artery disease. By combining NIRS with IVUS or OCT, the vascular inflammatory milieu and lipid-rich coronary plaque composition can be further visualized.^{22–26} Meanwhile, several studies have employed an intravascular NIRS system for detecting lipid core-containing plaques in vivo.^{22,27,28} Nevertheless, the development of intravascular NIRS still has limitations on miniaturized catheters and high spectral resolution.

Raman spectroscopy offers contrast specific to molecules from vibrations of chemical bonds in a noninvasive manner. Owing to the inelastic light scattering processes, Raman spectroscopy has been used to examine different biomolecules in the fingerprint region at 400–1800 cm^{-1} and high wavenumber region at 2400–3800 cm^{-1} .^{29–31} In particular, Raman spectroscopy has been applied to quantify the amounts of cholesterol, cholesterol esters, triglycerides and phospholipids, and calcium salts in intact tissue in human coronary arteries.³² To further achieve in vivo diagnosis, various fiber-optic Raman probes have been developed to characterize the atherosclerotic plaques and obtain information about the biochemical composition of the affected tissues.³⁰ Due to the miniature size of the instruments³³ and high collection efficiency,³⁴ intravascular Raman spectroscopy has greatly improved the risk assessment and management of coronary atherosclerosis as a robust diagnostic system.

In this review, we will focus on the instrumentation employed in intravascular Raman systems, especially fabrication strategies of fiber-optic Raman probes, and review their potential application for coronary atherosclerotic plaque

diagnosis and therapeutic strategies, the study of coronary atherosclerosis and plaques in vitro, preclinical intravascular detection of coronary atherosclerosis and plaques in vivo, and Raman spectroscopy study of coronary atherosclerosis and plaques in humans. Finally, we discuss the pros and cons of coronary atherosclerosis and atherosclerotic plaque detection by using label-free fiber-optic Raman probe spectroscopy. Furthermore, we will discuss the potential future direction on instrumentation and application of intravascular Raman in the future.

■ RAMAN SPECTROSCOPY FOR CORONARY ATHEROSCLEROSIS AND PLAQUE APPLICATIONS

Spontaneous Raman Spectroscopy System with a Miniaturized Raman Probe. Raman spectroscopy is a valuable optical technique that relies on the scattering of light regarding the vibrational modes of the molecules. Raman spectra can be acquired using near-infrared or visible light, such as 532 nm, 785 nm, 830 nm, and 1064 nm, to provide a relatively low fluorescent background and relatively good Raman signal-to-noise ratio (SNR) at 785 nm.³⁵ Accordingly, Raman spectroscopy has been widely used for biomedical diagnostics in various diseases.^{18,36} Nevertheless, due to the weak signal, Raman spectroscopy with bulky optical setups and long acquisition time has hindered its application in in vivo medical diagnosis. To address these problems, recent technical advancements have been achieved in translating Raman spectroscopy into real time in vivo detection tools. As an alternative to the gas and liquid laser counterparts, the diode laser can serve as a smaller, cost-effective substitute, greatly reducing the size and complexity of Raman systems.³⁷ On the other hand, the development of a fiber-optic Raman probe has enabled the improvement of SNR. For example, the Huang group has developed a 300 μm fiber-optic Raman needle probe, which is the thinnest Raman probe and has been successfully demonstrated to be suitable for acquiring high SNR in vivo fingerprint/high-wavenumber Raman spectra of deep organ tissues and biofluids within subseconds.³⁵

At present, there are three ways to realize Raman probes (Figure 1). First, based on proximal filters from tissue samples, the Raman fiber probe was realized as commercial equipment to detect the Raman signal of tissues in vitro. Although the

fiber background can be filtered, the outer diameter of the probe is limited to 5–10 mm, making it difficult to achieve intravascular detection in vivo (Figure 1a). Second, by coating excitation and collecting multimode fibers, it allows the Raman probe to be inserted into the endoscope working channel and placed in gentle contact with the tissue for real time in vivo biomedical applications (Figure 1b). With a core diameter of 200–400 μm , this method can achieve a smaller outer diameter within 1–5 mm. In this regard, the background of the coating at the tips of fibers would occur below 1000 cm^{-1} . Third, based on remote filters from tissue samples, an outer diameter of less than 1 mm can be achieved (Figure 1c). For example, Huang et al. developed a submillimeter fiber-optic Raman needle probe with 0.3 mm outside diameter³³ and coaxial double-clad-fiber and graded-index fiber-optic Raman probe at 0.14 mm³⁸ to acquire high-quality in vivo Raman spectra from various tissues, realizing the diagnosis and characterization of minimally invasive deep organ tissue and body biofluids in vivo (Figure 2). Nevertheless, this method has limited fiber length under 30 cm and can be affected by the Raman and fluorescent background of a single fiber. By using the appropriate spectral fitting algorithm, the interference of fiber-optic Raman and fluorescence backgrounds can be

effectively eliminated to keep enough SNR for tissue measurements.³³

By utilizing a quantitative optical design strategy, researchers developed a small-diameter and high-throughput Raman probe to optimize the collection efficiency and minimize the noise, which can be used on turbid samples and is able to provide access to remote tissues for spectroscopic evaluation.³⁹ The key parts were minimizing the fiber background and maximizing the collection efficiency under the safety conditions.⁴⁰ (1) The collection efficiency with a cooled spectrometer must be high enough to measure the weak tissue Raman signal along with a strong tissue intrinsic fluorescent signal in vivo within a short acquisition time ($<1\text{ s}$). A proper laser excitation power with a good SNR needs to be permitted by the American National Standards Institute (ANSI) standard. (2) By employing the use of fiber bundles, the proximal end of the fiber bundle that is attached to the spectrometer can be rearranged into a proper geometric shape (rectangle shape) to compensate for image aberration in the spectrograph, leading to a marked improvement in SNR with a short acquisition time.^{34,37} (3) To suppress the fiber background interference, there is a band-pass filter for laser excitation of filtered Raman probes. To suppress the Rayleigh scattered light, there is a long-pass filter for Raman signal collection. (4) Multiple collection fibers from 2 to 8 could increase the Raman signal collection area with maximizing collection efficiency.

The Raman fiber background is several magnitudes smaller compared to the weak tissue Raman signals. Sources of the fiber background include Raman signals from the fused-silica cores and fluorescence from dopants used or impurities present in the excitation fiber, which could get scattered back into the collection fiber of the Raman probe by the tissue. A band-pass filter for laser excitation was used to filter out the background, and a long-pass for Raman signal collection was used to filter out the Rayleigh scattered light of excitation laser. Deposited filters on the fiber tip could filter out most of the background but still keep some signals from 0 to 1200 cm^{-1} . The Huang group developed the fiber-optic Raman probe with coating excitation and collection fibers.^{41,42} The usage of filters on the fiber tip is a feasible and compact method to remove the unwanted background and Rayleigh scattered light, by separately coating the excitation and collection fibers of the Raman probe. By combining Raman spectroscopy with endoscopic imaging techniques as well as presenting a fiber-optic ball lens Raman probe, the interference of the fluorescence background and silica Raman in fiber can be effectively eliminated, while the Raman signal from tissues was collected to the maximum extent.^{34,43} The use of a large-pitch Kagome-lattice hollow-core photonic crystal fiber probe, transmitted through air inside the hollow core, significantly reduced the silica luminescence background by over 2 orders of magnitude as compared to standard silica fiber probes.⁴⁴ Moreover, a novel beveled fiber-optic confocal Raman probe coupled with a ball lens has been developed to enhance in vivo epithelial tissue Raman measurements at endoscopy^{42,45} (Figure 3).

Taken together, owing to its chemical selectivity and label-free capability, Raman spectroscopy with a fiber-optic Raman probe currently permits real time retrieval of different tissue characterization, biomedical diagnosis, and disease monitoring, opening new avenues to improve critical intravascular diagnostic information for better clinical decision-making.

Raman Spectroscopy Study of Coronary Atherosclerosis and Plaques in Vitro. Raman spectroscopy has, in

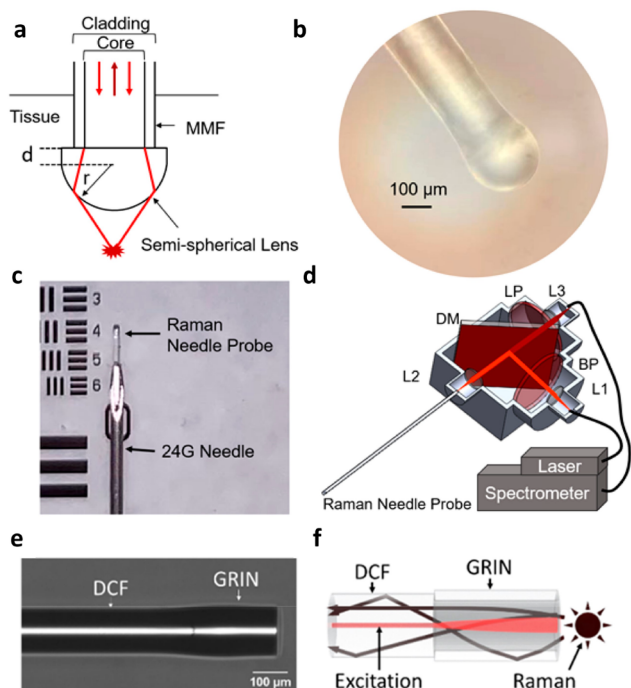


Figure 2. (a) Optical diagram of the submillimeter fiber-optic Raman needle probe tapered with a semispherical lens; (b) photograph of the submillimeter fiber-optic Raman needle probe fabricated (scale bar: $100\ \mu\text{m}$); (c) photograph of the submillimeter fiber-optic Raman needle probe inserted into a 24G syringe needle with USAF 1951 1 \times (Edmund Optics Inc.); (d) schematic of the fiber-optic Raman needle probe coupled with an optical filtering module and a laser Raman spectroscopy system. MMF: multimode fiber; BP: bandpass filter; LP: long-pass filter; DM: dichroic mirror; L: lens. (e) Microscopic image of the coaxial DCF-GRIN fiber-optic Raman probe. (f) Ray tracings of the excitation light and backscattered tissue Raman photons in the DCF-GRIN fiber-optic Raman probe. DCF: double-clad fiber; GRIN: graded index. (a–d) Adapted with permission from ref 33. Copyright [2021] Optical Society of America. (e, f) Adapted with permission from ref 38. Copyright [2022] Optical Society of America.

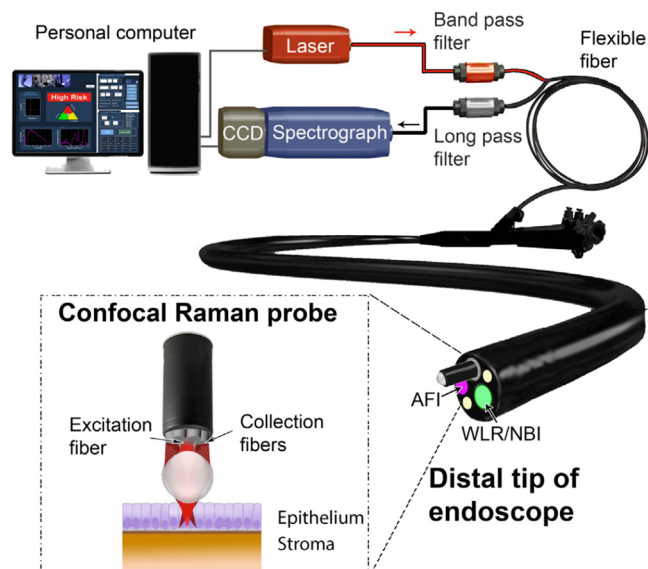


Figure 3. Rapid fiber-optic confocal Raman spectroscopy system developed for in vivo epithelial tissue diagnosis and characterization at endoscopy. Adapted with permission from ref 45. Copyright [2014] Gastroenterology.

recent years, developed a growing interest in the study of intravascular diseases because of the opportunity it provides for detecting biochemical changes with minimal invasiveness. This

technique has been used not only for understanding the pathophysiology behind the diseases but also for diagnosing the disease by detecting specific biomarkers. Especially, the wealth of biochemical information that can be uncovered by Raman spectroscopy in coronary atherosclerosis and plaques has been reported widely. In early 1998, Romer et al. demonstrated that the cholesterol content of a lesion can be determined by properly accounting for its depth into an arterial wall by using Raman spectroscopy.⁴⁶ Raman microscopy further offers a promising tool for easy and fast molecular imaging of discriminated cholesterol esters, cholesterol, and triglycerides in atherosclerosis⁴⁷ (Figure 4). Specifically, Raman bands at 699, 1298, 1438, 1669, 1729, and 2885 cm^{-1} were assigned to cholesterol esters as the main plaque compound, while Raman bands at 1061, 1126, 1297, 1439, 1740, and 2881 cm^{-1} were assigned to triglycerides in the perivascular lipid tissue.

By combining Raman spectroscopy with other methodologies, the mechanism involved in pathogenesis of atherosclerotic plaque has been discovered. Romer et al. explored the information about the chemical composition of an artery wall obtained with Raman spectroscopy and morphological information generated with IVUS to localize and quantify cholesterol and calcium salt deposits in intact arterial walls in vitro.⁴⁸ By the combination of Raman and fluorescence spectroscopy, Haka et al. examined that the main forms of modified low-density lipoprotein detected in both the coronary artery and aortic plaques are peroxidation products from the

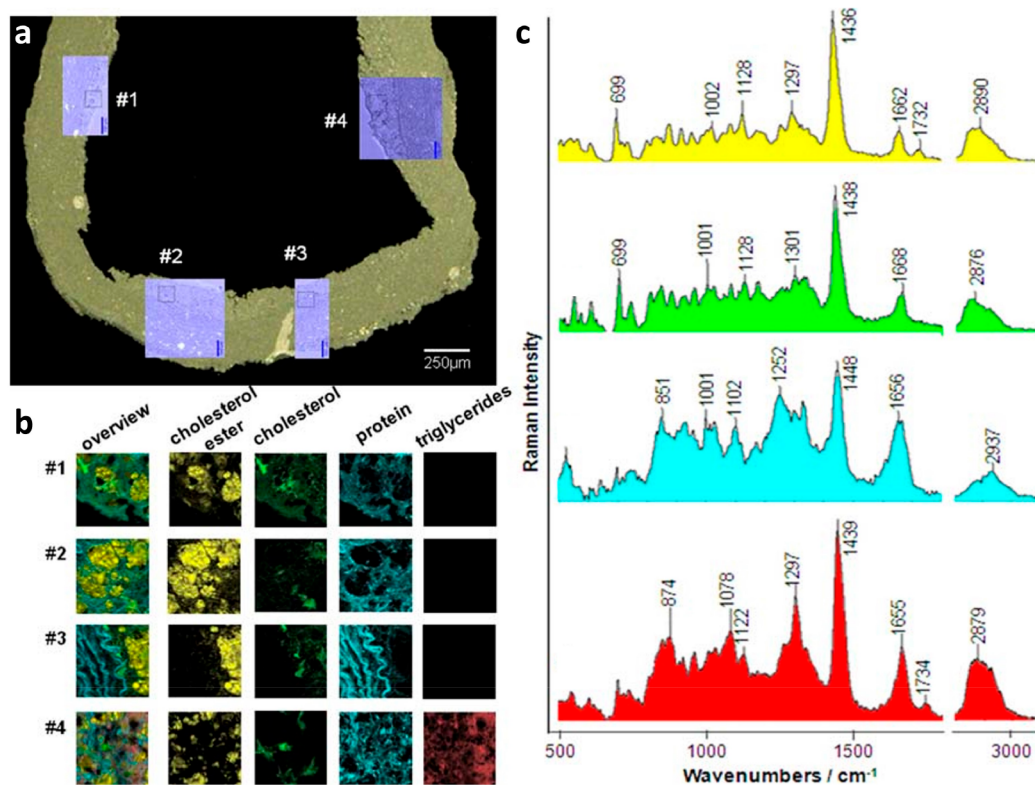


Figure 4. Raman microscopy of the thoracic aorta. (a) Unstained cross section of the thoracic aorta. (b) The intimal numbered marks, analyzed using a vertex component analysis algorithm, resulting in the corresponding pseudocolor maps of $100 \times 100 \mu\text{m}$. Overview images and specification of the main components (cholesterol esters, cholesterol, triglycerides, and protein compounds of the connective tissue) are shown. (c) The corresponding spectra are plotted according to the Raman image color-code in (b). Adapted with permission from ref 47. Copyright [2013] Journal of Biophotonics.

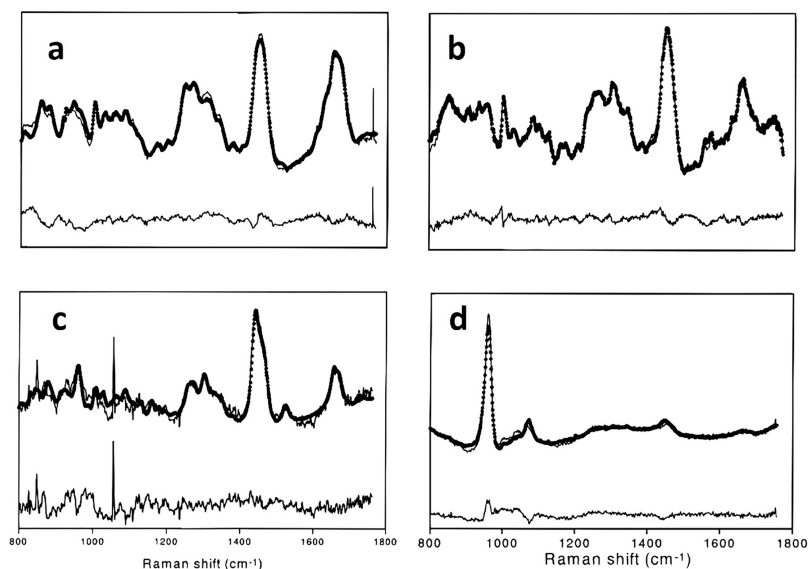


Figure 5. Examples of transmurally collected Raman spectra using fiber-optic probes that were modeled to obtain molecular information from the examined site. (a) and (b) show spectra collected in vivo from the aortic wall with a forward-viewing probe (10 s) and the iliac artery with a side-viewing probe (30 s), respectively. (c) and (d) show spectra of a noncalcified atherosclerotic plaque (10 s) and a calcified atherosclerotic plaque (10 s), respectively, collected in buffer perfused human coronary artery in vitro using side-viewing probes. Residuals (data minus fitted spectrum) of the fits are shown on the same scale. Experimental conditions: power, 100 mW. Adapted with permission from ref 53. Copyright [2000] American Chemical Society.

Fenton reaction and myeloperoxidase–hypochlorite pathway,⁴⁹ which provides insight into the pathogenesis of atherosclerosis. The combination of diffuse reflectance spectroscopy, intrinsic fluorescence spectroscopy, and Raman spectroscopy can provide detailed biochemical information about the disease state of the plaque tissue and detect vulnerable plaque characteristics.⁵⁰ Moreover, Marzec et al. described a methodology with the use of Raman spectroscopy, infrared spectroscopy, and atomic force microscopy to visualize the different features of protein and lipid in atherosclerotic plaque.⁵¹ By using the multimodal fluorescence lifetime imaging–Raman data set, the accumulation of low-density lipoprotein has been identified as the primary source of lifetime contrast in atherosclerotic lesions.⁵²

Taken together, Raman spectroscopy is a desirable approach to study plaque biology in atherosclerosis, providing great potential in the early diagnosis of disease, monitoring of therapy efficacy, and investigation of disease pathogenesis.

Preclinical Intravascular Detection of Coronary Atherosclerosis and Plaques in Vivo. Although the potential mechanism in normal and diseased arteries in vitro has been discovered by Raman spectroscopy, the complexity of traditional confocal spectroscopy equipment limits its application in coronary atherosclerosis and plaques intravascularly to some extent. Along with the development of the fiber-optic Raman probe spectroscopy system, this technique has been widely used in intravascular coronary arteries.

In early 2000, Buschman et al. measured the composition of the artery wall and determined the type of atherosclerotic plaques using an intravascular miniaturized fiber-optic Raman probe.⁵³ By comparing the spectrum of the aortic wall and iliac artery in vivo (Figure 5a,b) and a noncalcified atherosclerotic plaque and a calcified atherosclerotic plaque in vitro (Figure 5c,d), the study showed that in-vivo-collected aorta spectra are a simple summation of signal contributions of the aortic wall and blood (with signal contributions primarily due to

hemoglobin and water). By the development of efficient, high-throughput, low-background optical fiber Raman probes, researchers present an in vivo tissue analysis that is capable of collecting and processing Raman spectra in less than 2 s.⁵⁴ With this technique, they reported the evidence that Raman spectroscopy has the potential to identify vulnerable plaque, achieving a sensitivity and specificity of 79 and 85%, respectively.⁵⁵ Taken together, these studies demonstrated the sensitivity of an intravascular Raman probe to identify spectroscopic features associated with plaque vulnerability, including the major molecular composition of cholesterol, the lipid core, calcification, elastic lamina, adventitial fat, and collagen. A comprehensive overview of all discussed intravascular Raman system parameters is summarized in Table 1.

In contrast to other modalities, Raman spectroscopy offers enormous benefits because of its potential to provide quantitative data. Early on in cardiovascular applications with Raman spectroscopy, it was demonstrated that individual plaque components can be quantified. Because of the unique compositional parameters, different plaque types can be

Table 1. Device Parameters of Raman Spectroscopy in Vivo

Laser wavelength	Outer diameter	Detection range	Spectral resolution	Reference
830 nm	NA ^a	750–1800 cm ⁻¹	10 cm ⁻¹	53
830 nm	NA ^a	686–1788 cm ⁻¹	9.4 cm ⁻¹	54, 55
785 nm	1.8 mm	800–1800 cm ⁻¹	9 cm ⁻¹	41
785 nm	1 mm	0–3500 cm ⁻¹	NA	56
785 nm	5 mm	800–1800 cm ⁻¹ 2800–3700 cm ⁻¹	8 cm ⁻¹	57

^aNA: the parameter was not available.

analyzed in a nonsubjective manner that can assist in the recognition of vulnerable plaques and improve the aforementioned risk management. In order to reveal the chemical composition and spatial distribution simultaneously, experiments in combination with other imaging techniques, in particular, with coherent anti-Stokes Raman scattering and OCT, have demonstrated that Raman spectroscopy is extremely sensitive to intravascular detection of coronary arteries. For example, researchers developed a miniaturized filtered probe with one excitation and 12 collection fibers integrated in a 1 mm sleeve to detect varying amounts of plaque depositions, with *in vivo* characterization of atherosclerotic plaque depositions by Raman probe spectroscopy and *in vitro* coherent anti-Stokes Raman scattering microscopic imaging on a rabbit model.⁵⁶ By combining Raman spectroscopy with OCT for the characterization of plaques on rabbits *in vivo*, the spectral information and intravascular morphology were obtained simultaneously, which identified plaque depositions consisting of lipids, with triglyceride as the major component.⁵⁸ In particular, the multiplexed surface-enhanced Raman scattering (SERS) based molecular imaging can indicate the status of vascular inflammation *in vivo* and gives promise for SERS as a clinical imaging technique for cardiovascular disease in the future.⁵⁹

Collectively, with enough information regarding spectral composition and intravascular morphology, Raman spectroscopy with fiber-optic probes has great potential to investigate plaque developments and treatments, which opens new avenues for facilitating the adoption of Raman spectroscopy into clinical research and practice.

Raman Spectroscopy Study of Coronary Atherosclerosis and Plaques in Humans. Raman spectroscopy can provide a wealth of biochemical information, making it a promising tool for studying coronary atherosclerosis and plaques in humans. For example, Feld's group has acquired Raman spectra in an early *in situ* study involving nine explanted recipient hearts. In this study, researchers quantified the relative amounts of biochemicals present in the coronary artery, including cholesterol, cholesterol esters, triglycerides, phospholipids, and calcium salts.³² They subsequently developed a diagnostic algorithm, based on a set of 97 human coronary artery samples, that demonstrated a strong correlation of the relative weights of cholesterol and calcium salts with histological diagnoses of the same locations.⁶⁰ The algorithm was then tested prospectively in a second validation human data set and correctly classified 64 of 69 coronary artery samples.⁶¹ By combining diffuse reflectance spectroscopy, intrinsic fluorescence spectroscopy, and Raman spectroscopy, a novel method named multimodal spectroscopy (MMS), the group demonstrated the depth-sensitive and complementary morphological information about vulnerable plaque features, including a thin fibrous cap, necrotic core, superficial foam cells, and thrombus.^{50,62} By using MMS, suspected vulnerable plaques can be detected with a sensitivity of 96% and specificity of 72%.⁵⁰ In addition, another algorithm using principal component analysis and discriminant analysis has been developed and successfully applied to diagnose coronary artery disease by Raman spectroscopy with good sensitivity and specificity.⁶³ Taking advantage of Fourier-transform Raman spectroscopy to reduce the effects of tissue fluorescence and promote less photolytic degradation of samples, researchers have identified and classified the tissues found in the atherosclerotic process in human carotid *in*

vitro.⁶⁴ This method has the ability to identify alterations to the diffuse thickening of the intima layer and classify it depending on the intensity of the thickening. Furthermore, Chau et al. used fingerprint and high-wavenumber Raman spectroscopy in a human-swine coronary xenograft *in vivo*, to identify the morphology and chemical composition of the artery wall.⁶⁵ By comparing Raman and fluorescence lifetime spectroscopy from human atherosclerotic lesions using a bimodal probe, Popp et al. found that Raman spectroscopy could distinguish lipid from necrotic cores, whereas fluorescence lifetime imaging extracted information could identify fibrous caps.⁶⁶

Taken together, the chemical information that Raman spectroscopy provided makes it a useful tool for monitoring the progression and regression of atherosclerosis, predicting plaque rupture, and selecting proper therapeutic intervention. In the future, we expect the development of Raman spectroscopy with better Raman probes, realizing real clinical applications.

CONCLUSION AND DISCUSSION

The major use for vibrational spectroscopy as a clinical diagnostic tool can be screening biological fluids or biopsy samples for disease-specific molecular signatures. In particular, by combining transmission Raman spectroscopy and ultra-bright surface-enhanced Raman scattering nanotags, the Ye group has developed a Raman detection system with deep-detection capability and clinical photosafety to realize *in vivo* imaging of "phantom" lesions labeled by nanotags in a 1.5 cm thick unshaved mouse under permissible exposure.⁶⁷ Moreover, in order to improve the SNR, the Raman spectral denoising algorithms have been commonly used.³¹ For instance, machine intelligent and deep learning methods were developed to improve the accuracy and robustness of spectral classification by Raman spectroscopy.^{68,69} Huang et al. developed a Raman-specified convolutional neural network, for the diagnosis of nasopharyngeal carcinoma and assessment of post-treatment efficacy.⁷⁰ More recently, by using the binary stochastic filtering in the deep learning method, Xun et al. analyzed the contribution of Raman spectra and found the contribution molecules such as glucose, collagen and protein, nucleic acids, saturated and unsaturated fatty acid, and lipids in representative Raman data sets.⁷¹ With the minimization of photon damage and the improvements of SNR, an *in vivo* Raman biopsy has become possible for clinical application.

Much progress is being made in developing vibrational spectroscopy for imaging intravascular diseases, and vibrational techniques are still at the proof-of-concept stage of preclinical development.^{30,39,72} Advances in medical devices have enabled the construction of a suite of multimodality, intravascular imaging, and component quantification catheters that can provide comprehensive visualization of plaque pathophysiology and biology. Owing to the capability of detecting molecular information, fiber-optic Raman endoscopy has become a powerful tool for *in vivo* disease monitoring and tissue characterization, in particular, identifying the spectral features of plaque vulnerability and vascular inflammation. We believe technical advancements in Raman spectroscopy would further promote the research field of coronary atherosclerosis and plaque diagnosis. First, one limitation of the Raman probes used is that they do not provide a real-time image of the vessel wall in the way that IVUS and OCT do. Therefore, the addition of Raman probes on the imaged multimodal catheter

with improved sensitivity and specificity could allow quantitative mapping of the biochemistry of the plaque and provide in vivo, label-free diagnosis of atherosclerosis. Second, machine intelligence methods (machine learning, manifold learning, and deep learning) can be developed in the future to observe subtle spectral differences to improve the accuracy and robustness of Raman spectral classification. Third, the Raman signal can be further improved to avoid the influence of blood flow, for example, by focusing the probe front focus for deeper detection or by using algorithms to remove blood flow background. Looking into the future, Raman spectroscopy will further improve our understanding of plaque pathophysiology and biology and provide significant promise for label-free in vivo diagnostics.

AUTHOR INFORMATION

Corresponding Authors

Xun Chen – Key Laboratory of Biomechanics and Mechanobiology (Beihang University), Ministry of Education, Institute of Medical Photonics, Beijing Advanced Innovation Center for Biomedical Engineering, School of Biological Science and Medical Engineering, Beihang University, Beijing 100191, China; orcid.org/0009-0001-4351-367X; Email: chenxun2007@buaa.edu.cn

Peipei Hou – Department of Cardiology, The People's Hospital of China Medical University, Shenyang 110016, China; Email: happy1982630@163.com

Shuhua Yue – Key Laboratory of Biomechanics and Mechanobiology (Beihang University), Ministry of Education, Institute of Medical Photonics, Beijing Advanced Innovation Center for Biomedical Engineering, School of Biological Science and Medical Engineering, Beihang University, Beijing 100191, China; orcid.org/0000-0003-1830-008X; Email: yue_shuhua@buaa.edu.cn

Authors

Hao Jia – Key Laboratory of Biomechanics and Mechanobiology (Beihang University), Ministry of Education, Institute of Medical Photonics, Beijing Advanced Innovation Center for Biomedical Engineering, School of Biological Science and Medical Engineering, Beihang University, Beijing 100191, China; orcid.org/0000-0003-0146-6171

Jianghao Shen – Key Laboratory of Biomechanics and Mechanobiology (Beihang University), Ministry of Education, Institute of Medical Photonics, Beijing Advanced Innovation Center for Biomedical Engineering, School of Biological Science and Medical Engineering, Beihang University, Beijing 100191, China

Rujia Liu – Key Laboratory of Biomechanics and Mechanobiology (Beihang University), Ministry of Education, Institute of Medical Photonics, Beijing Advanced Innovation Center for Biomedical Engineering, School of Biological Science and Medical Engineering, Beihang University, Beijing 100191, China

Complete contact information is available at: <https://pubs.acs.org/10.1021/acsomega.4c01611>

Author Contributions

H.J. contributed to the systematic review of the literature and wrote the initial draft of the manuscript. J.S. and R.L. summarized the techniques of Raman spectroscopy. S.Y., X.C., and P.H. modified the review article and critically analyzed and approved it.

Notes

The authors declare no competing financial interest.

ACKNOWLEDGMENTS

This work was supported by National Natural Science Foundation of China (No. U23B2046, No. 62027824, and No. 62205010); Beijing Natural Science Foundation (No. 7224367 and No. L223018); and Fundamental Research Funds for the Central Universities (No. YWF-22-L-547 and No. YWF-22-L-1265).

REFERENCES

- (1) Gaba, P.; Gersh, B. J.; Muller, J.; Narula, J.; Stone, G. W. Evolving concepts of the vulnerable atherosclerotic plaque and the vulnerable patient: implications for patient care and future research. *Nature reviews. Cardiology* **2023**, *20* (3), 181–196.
- (2) Otsuka, F.; Joner, M.; Prati, F.; Virmani, R.; Narula, J. Clinical classification of plaque morphology in coronary disease. *Nature reviews. Cardiology* **2014**, *11* (7), 379–89.
- (3) Mintz, G. S.; Guagliumi, G. Intravascular imaging in coronary artery disease. *Lancet* **2017**, *390* (10096), 793–809.
- (4) Garcia-Garcia, H. M.; Jang, I. K.; Serruys, P. W.; Kovacic, J. C.; Narula, J.; Fayad, Z. A. Imaging plaques to predict and better manage patients with acute coronary events. *Circulation research* **2014**, *114* (12), 1904–17.
- (5) Bourantas, C. V.; Jaffer, F. A.; Gijssen, F. J.; van Soest, G.; Madden, S. P.; Courtney, B. K.; Fard, A. M.; Tenekecioglu, E.; Zeng, Y.; van der Steen, A. F. W.; Emelianov, S.; Muller, J.; Stone, P. H.; Marcu, L.; Tearney, G. J.; Serruys, P. W. Hybrid intravascular imaging: recent advances, technical considerations, and current applications in the study of plaque pathophysiology. *Eur. Heart J.* **2017**, *38* (6), 400–412.
- (6) McDaniel, M. C.; Eshtehardi, P.; Sawaya, F. J.; Douglas, J. S.; Samady, H. Contemporary Clinical Applications of Coronary Intravascular Ultrasound. *JACC: Cardiovascular Interventions* **2011**, *4* (11), 1155–1167.
- (7) Garcia-Garcia, H. M.; Costa, M. A.; Serruys, P. W. Imaging of coronary atherosclerosis: intravascular ultrasound. *European Heart Journal* **2010**, *31* (20), 2456–2469.
- (8) Wang, L.; Zhao, Y.; Zheng, B.; Huo, Y.; Fan, Y.; Ma, D.; Gu, Y.; Wang, P. Ultrawide-bandwidth high-resolution all-optical intravascular ultrasound using miniaturized photoacoustic transducer. *Science advances* **2023**, *9* (23), No. eadg8600.
- (9) Li, B. H.; Leung, A. S. O.; Soong, A.; Munding, C. E.; Lee, H.; Thind, A. S.; Munce, N. R.; Wright, G. A.; Rowsell, C. H.; Yang, V. X. D.; Strauss, B. H.; Stuart Foster, F.; Courtney, B. K. Hybrid intravascular ultrasound and optical coherence tomography catheter for imaging of coronary atherosclerosis. *Catheterization and Cardiovascular Interventions* **2013**, *81* (3), 494–507.
- (10) Xiang Li; Jiawen Li; Jing, J.; Teng Ma; Shanshan Liang; Jun Zhang; Mohar, D.; Raney, A.; Mahon, S.; Brenner, M.; Patel, P.; Shung, K. K.; Qifa Zhou; Zhongping Chen. Integrated IVUS-OCT Imaging for Atherosclerotic Plaque Characterization. *IEEE J. Sel. Top. Quantum Electron.* **2014**, *20* (2), 196–203.
- (11) Ono, M.; Kawashima, H.; Hara, H.; Gao, C.; Wang, R.; Kogame, N.; Takahashi, K.; Chichareon, P.; Modolo, R.; Tomiani, M.; Wykrzykowska, J. J.; Piek, J. J.; Mori, L.; Courtney, B. K.; Wijns, W.; Sharif, F.; Bourantas, C.; Onuma, Y.; Serruys, P. W. Advances in IVUS/OCT and Future Clinical Perspective of Novel Hybrid Catheter System in Coronary Imaging. *Frontiers in Cardiovascular Medicine* **2020**, DOI: [10.3389/fcvm.2020.00119](https://doi.org/10.3389/fcvm.2020.00119).
- (12) Falk, E.; Shah, P. K.; Fuster, V. Coronary plaque disruption. *Circulation* **1995**, *92* (3), 657–71.
- (13) Libby, P. Lesion versus lumen. *Nature medicine* **1995**, *1* (1), 17–8.
- (14) Kramer, C. M. The vulnerable atherosclerotic plaque: strategies for diagnosis and management. *Circulation* **2007**, DOI: [10.1161/CIRCULATIONAHA.107.694349](https://doi.org/10.1161/CIRCULATIONAHA.107.694349).

- (15) Jaffer, F. A.; Calfon, M. A.; Rosenthal, A.; Mallas, G.; Razansky, R. N.; Mausekapp, A.; Weissleder, R.; Libby, P.; Ntziachristos, V. Two-dimensional intravascular near-infrared fluorescence molecular imaging of inflammation in atherosclerosis and stent-induced vascular injury. *J. Am. Coll. Cardiol.* **2011**, *57* (25), 2516–26.
- (16) Vinegoni, C.; Botnaru, I.; Aikawa, E.; Calfon, M. A.; Iwamoto, Y.; Folco, E. J.; Ntziachristos, V.; Weissleder, R.; Libby, P.; Jaffer, F. A. Indocyanine green enables near-infrared fluorescence imaging of lipid-rich, inflamed atherosclerotic plaques. *Science translational medicine* **2011**, *3* (84), No. 84ra45.
- (17) Bec, J.; Vela, D.; Phipps, J. E.; Agung, M.; Unger, J.; Margulies, K. B.; Southard, J. A.; Buja, L. M.; Marcu, L. Label-Free Visualization and Quantification of Biochemical Markers of Atherosclerotic Plaque Progression Using Intravascular Fluorescence Lifetime. *JACC. Cardiovascular imaging* **2021**, *14* (9), 1832–1842.
- (18) Kumar, S.; Verma, T.; Mukherjee, R.; Ariese, F.; Somasundaram, K.; Umopathy, S. Raman and infra-red micro-spectroscopy: towards quantitative evaluation for clinical research by ratiometric analysis. *Chem. Soc. Rev.* **2016**, *45* (7), 1879–900.
- (19) Caplan, J. D.; Waxman, S.; Nesto, R. W.; Muller, J. E. Near-infrared spectroscopy for the detection of vulnerable coronary artery plaques. *J. Am. Coll. Cardiol.* **2006**, *47* (8), C92–6.
- (20) Schuurman, A.-S.; Vroegindewey, M.; Kardys, I.; Oemrawsingh, R. M.; Cheng, J. M.; de Boer, S.; Garcia-Garcia, H. M.; van Geuns, R.-J.; Regar, E. S.; Daemen, J.; van Mieghem, N. M.; Serruys, P. W.; Boersma, E.; Akkerhuis, K. M. Near-infrared spectroscopy-derived lipid core burden index predicts adverse cardiovascular outcome in patients with coronary artery disease during long-term follow-up. *European Heart Journal* **2018**, *39* (4), 295–302.
- (21) Oemrawsingh, R. M.; Cheng, J. M.; Garcia-Garcia, H. M.; van Geuns, R.-J.; de Boer, S. P. M.; Simsek, C.; Kardys, I.; Lenzen, M. J.; van Domburg, R. T.; Regar, E.; Serruys, P. W.; Akkerhuis, K. M.; Boersma, E. Near-Infrared Spectroscopy Predicts Cardiovascular Outcome in Patients With Coronary Artery Disease. *Journal of the American College of Cardiology* **2014**, *64* (23), 2510–2518.
- (22) Pu, J.; Mintz, G. S.; Brilakis, E. S.; Banerjee, S.; Abdel-Karim, A. R.; Maini, B.; Biro, S.; Lee, J. B.; Stone, G. W.; Weisz, G.; Maehara, A. In vivo characterization of coronary plaques: novel findings from comparing greyscale and virtual histology intravascular ultrasound and near-infrared spectroscopy. *Eur. Heart J.* **2012**, *33* (3), 372–83.
- (23) de Boer, S. P.; Brugaletta, S.; Garcia-Garcia, H. M.; Simsek, C.; Heo, J. H.; Lenzen, M. J.; Schultz, C.; Regar, E.; Zijlstra, F.; Boersma, E.; Serruys, P. W. Determinants of high cardiovascular risk in relation to plaque-composition of a non-culprit coronary segment visualized by near-infrared spectroscopy in patients undergoing percutaneous coronary intervention. *Eur. Heart J.* **2014**, *35* (5), 282–9.
- (24) Waksman, R.; Di Mario, C.; Torguson, R.; Ali, Z. A.; Singh, V.; Skinner, W. H.; Artis, A. K.; Cate, T. T.; Powers, E.; Kim, C.; Regar, E.; Wong, S. C.; Lewis, S.; Wykrzykowska, J.; Dube, S.; Kazzaha, S.; van der Ent, M.; Shah, P.; Craig, P. E.; Zou, Q.; Kolm, P.; Brewer, H. B.; Garcia-Garcia, H. M.; Samady, H.; Tobis, J.; Zainea, M.; Leimbach, W.; Lee, D.; Lalonde, T.; Skinner, W.; Villa, A.; Liberman, H.; Younis, G.; de Silva, R.; Diaz, M.; Tami, L.; Hodgson, J.; Raveendran, G.; Goswami, N.; Arias, J.; Lovitz, L.; Carida, R.; Potluri, S.; Prati, F.; Erglis, A.; Pop, A.; McEntegart, M.; Hudec, M.; Rangasetty, U.; Newby, D. Identification of patients and plaques vulnerable to future coronary events with near-infrared spectroscopy intravascular ultrasound imaging: a prospective, cohort study. *Lancet* **2019**, *394* (10209), 1629–1637.
- (25) Gyldenkerne, C.; Maeng, M.; Kjoller-Hansen, L.; Maehara, A.; Zhou, Z.; Ben-Yehuda, O.; Erik Botker, H.; Engstrom, T.; Matsumura, M.; Mintz, G. S.; Fröbert, O.; Persson, J.; Wiseth, R.; Larsen, A. I.; Jensen, L. O.; Nordrehaug, J. E.; Bleie, Ø.; Omerovic, E.; Held, C.; James, S. K.; Ali, Z. A.; Rosen, H. C.; Stone, G. W.; Erlinge, D. Coronary Artery Lesion Lipid Content and Plaque Burden in Diabetic and Nondiabetic Patients: PROSPECT II. *Circulation* **2023**, *147* (6), 469–481.
- (26) Shimokado, A.; Kubo, T.; Nishiguchi, T.; Katayama, Y.; Taruya, A.; Ohta, S.; Kashiwagi, M.; Shimamura, K.; Kuroi, A.; Kameyama, T.; Shiono, Y.; Yamano, T.; Matsuo, Y.; Kitabata, H.; Ino, Y.; Hozumi, T.; Tanaka, A.; Akasaka, T. Automated lipid-rich plaque detection with short wavelength infra-red OCT system. *European heart journal. Cardiovascular Imaging* **2018**, *19* (10), 1174–1178.
- (27) Waxman, S.; Dixon, S. R.; L'Allier, P.; Moses, J. W.; Petersen, J. L.; Cutlip, D.; Tardif, J. C.; Nesto, R. W.; Muller, J. E.; Hendricks, M. J.; Sum, S. T.; Gardner, C. M.; Goldstein, J. A.; Stone, G. W.; Krucoff, M. W. In vivo validation of a catheter-based near-infrared spectroscopy system for detection of lipid core coronary plaques: initial results of the SPECTACL study. *JACC. Cardiovascular imaging* **2009**, *2* (7), 858–68.
- (28) Erlinge, D. Near-infrared spectroscopy for intracoronary detection of lipid-rich plaques to understand atherosclerotic plaque biology in man and guide clinical therapy. *Journal of Internal Medicine* **2015**, *278* (2), 110–125.
- (29) Talari, A. C. S.; Movasaghi, Z.; Rehman, S.; Rehman, I. u. Raman Spectroscopy of Biological Tissues. *Appl. Spectrosc. Rev.* **2015**, *50* (1), 46–111.
- (30) Cordero, E. In-vivo Raman spectroscopy: from basics to applications. *Journal of Biomedical Optics* **2018**, *23* (07), 1.
- (31) Fang, S.; Wu, S.; Chen, Z.; He, C.; Lin, L. L.; Ye, J. Recent progress and applications of Raman spectrum denoising algorithms in chemical and biological analyses: A review. *TrAC Trends in Analytical Chemistry* **2024**, *172*, 117578.
- (32) Brennan, J. F., 3rd; Römer, T. J.; Lees, R. S.; Tercyak, A. M.; Kramer, J. R., Jr.; Feld, M. S. Determination of human coronary artery composition by Raman spectroscopy. *Circulation* **1997**, *96* (1), 99–105.
- (33) Shu, C.; Zheng, W.; Wang, Z.; Yu, C.; Huang, Z. Development and characterization of a disposable submillimeter fiber optic Raman needle probe for enhancing real-time in vivo deep tissue and biofluids Raman measurements. *Opt. Lett.* **2021**, *46* (20), S197.
- (34) Mo, J.; Zheng, W.; Huang, Z. Fiber-optic Raman probe couples ball lens for depth-selected Raman measurements of epithelial tissue. *Biomedical optics express* **2010**, *1* (1), 17–30.
- (35) Pavel Matousek, M. D. M. *Emerging Raman applications and techniques in biomedical and pharmaceutical fields*; Springer, 2010.
- (36) Nicolson, F.; Kircher, M. F.; Stone, N.; Matousek, P. Spatially offset Raman spectroscopy for biomedical applications. *Chem. Soc. Rev.* **2021**, *50* (1), 556–568.
- (37) Huang, Z.; Zeng, H.; Hamzavi, I.; McLean, D. I.; Lui, H. Rapid near-infrared Raman spectroscopy system for real-time in vivo skin measurements. *Opt. Lett.* **2001**, *26* (22), 1782–4.
- (38) Heng, H. P. S.; Shu, C.; Zheng, W.; Huang, Z. Development of a coaxial DCF-GRIN fiberoptic Raman probe for enhancing in vivo epithelial tissue Raman measurements. *Opt. Lett.* **2022**, *47* (22), S989.
- (39) Motz, J. T.; Hunter, M.; Galindo, L. H.; Gardecki, J. A.; Kramer, J. R.; Dasari, R. R.; Feld, M. S. Optical fiber probe for biomedical Raman spectroscopy. *Applied optics* **2004**, *43* (3), 542–54.
- (40) Heng, H. P. S.; S, C.; Zheng, W.; Lin, K.; Huang, Z. Advances in real-time fiber-optic Raman spectroscopy for early cancer diagnosis: Pushing the frontier into clinical endoscopic applications. *Translational Biophotonics* **2020**, DOI: 10.1002/tbio.202000018.
- (41) Huang, Z.; Teh, S. K.; Zheng, W.; Mo, J.; Lin, K.; Shao, X.; Ho, K. Y.; Teh, M.; Yeoh, K. G. Integrated Raman spectroscopy and trimodal wide-field imaging techniques for real-time in vivo tissue Raman measurements at endoscopy. *Opt. Lett.* **2009**, *34* (6), 758–60.
- (42) Wang, J.; Bergholt, M. S.; Zheng, W.; Huang, Z. Development of a beveled fiber-optic confocal Raman probe for enhancing in vivo epithelial tissue Raman measurements at endoscopy. *Opt. Lett.* **2013**, *38* (13), 2321.
- (43) Day, J. C. C.; Bennett, R.; Smith, B.; Kendall, C.; Hutchings, J.; Meaden, G. M.; Born, C.; Yu, S.; Stone, N. A miniature confocal Raman probe for endoscopic use. *Phys. Med. Biol.* **2009**, *54* (23), 7077–7087.
- (44) Ghenuche, P.; Rammler, S.; Joly, N. Y.; Scharrer, M.; Frosz, M.; Wenger, J.; Russell, P. S.; Rigneault, H. Kagome hollow-core photonic crystal fiber probe for Raman spectroscopy. *Opt. Lett.* **2012**, *37* (21), 4371–3.

- (45) Bergholt, M. S.; Zheng, W.; Ho, K. Y.; Teh, M.; Yeoh, K. G.; Yan So, J. B.; Shabbir, A.; Huang, Z. Fiberoptic Confocal Raman Spectroscopy for Real-Time In Vivo Diagnosis of Dysplasia in Barrett's Esophagus. *Gastroenterology* **2014**, *146* (1), 27–32.
- (46) Romer, T. J.; Brennan III, J. F.; Bakker Schut, T. C.; Wolthuis, R.; van den Hoogen, R. C.M.; Emeis, J. J.; van der Laarse, A.; Bruschke, A. V.G.; Puppels, G. J. Raman spectroscopy for quantifying cholesterol in intact coronary artery wall. *Atherosclerosis* **1998**, *141* (1), 117–24.
- (47) Lattermann, A.; Matthäus, C.; Bergner, N.; Beleites, C.; Romeike, B. F.; Krafft, C.; Brehm, B. R.; Popp, J. Characterization of atherosclerotic plaque depositions by Raman and FTIR imaging. *Journal of Biophotonics* **2013**, *6* (1), 110–121.
- (48) Römer, T. J.; Brennan, J. F., 3rd; Puppels, G. J.; Zwinderman, A. H.; van Duinen, S. G.; van der Laarse, A.; van der Steen, A. F.; Bom, N. A.; Bruschke, A. V. Intravascular ultrasound combined with Raman spectroscopy to localize and quantify cholesterol and calcium salts in atherosclerotic coronary arteries. *Arterioscler., Thromb., Vasc. Biol.* **2000**, *20* (2), 478–83.
- (49) Haka, A. S.; Kramer, J. R.; Dasari, R. R.; Fitzmaurice, M. Mechanism of ceroid formation in atherosclerotic plaque: in situ studies using a combination of Raman and fluorescence spectroscopy. *Journal of Biomedical Optics* **2011**, *16* (1), 011011.
- (50) Šćepanović, O. R.; Fitzmaurice, M.; Miller, A.; Kong, C.-R.; Volynskaya, Z.; Dasari, R. R.; Kramer, J. R.; Feld, M. S. Multimodal spectroscopy detects features of vulnerable atherosclerotic plaque. *Journal of Biomedical Optics* **2011**, *16* (1), 011009.
- (51) Marzec, K. M.; Wrobel, T. P.; Rygula, A.; Maslak, E.; Jaształ, A.; Fedorowicz, A.; Chlopicki, S.; Baranska, M. Visualization of the biochemical markers of atherosclerotic plaque with the use of Raman, IR and AFM. *Journal of Biophotonics* **2014**, *7* (9), 744–756.
- (52) Bec, J.; Shaik, T. A.; Krafft, C.; Bocklitz, T. W.; Alfonso-Garcia, A.; Margulies, K. B.; Popp, J.; Marcu, L. Investigating Origins of FLIm Contrast in Atherosclerotic Lesions Using Combined FLIm-Raman Spectroscopy. *Frontiers in Cardiovascular Medicine* **2020**, DOI: 10.3389/fcvm.2020.00122.
- (53) Buschman, H. P.; Marple, E. T.; Wach, M. L.; Bennett, B.; Bakker Schut, T. C.; Bruining, H. A.; Bruschke, A. V.; van der Laarse, A.; Puppels, G. J. In vivo determination of the molecular composition of artery wall by intravascular Raman spectroscopy. *Anal. Chem.* **2000**, *72* (16), 3771–3775.
- (54) Motz, J. T.; Gandhi, S. J.; Sćepanovic, O. R.; Haka, A. S.; Kramer, J. R.; Dasari, R. R.; Feld, M. S. Real-time Raman system for in vivo disease diagnosis. *Journal of Biomedical Optics* **2005**, *10* (3), 031113.
- (55) Motz, J. T.; Fitzmaurice, M.; Miller, A.; Gandhi, S. J.; Haka, A. S.; Galindo, L. H.; Dasari, R. R.; Kramer, J. R.; Feld, M. S. In vivo Raman spectral pathology of human atherosclerosis and vulnerable plaque. *J. Biomed Opt* **2006**, *11* (2), No. 021003.
- (56) Matthäus, C.; Dochow, S.; Bergner, G.; Lattermann, A.; Romeike, B. F. M.; Marple, E. T.; Krafft, C.; Dietzek, B.; Brehm, B. R.; Popp, J. In Vivo Characterization of Atherosclerotic Plaque Depositions by Raman-Probe Spectroscopy and in Vitro Coherent Anti-Stokes Raman Scattering Microscopic Imaging on a Rabbit Model. *Anal. Chem.* **2012**, *84* (18), 7845–7851.
- (57) Duraipandian, S.; Zheng, W.; Ng, J.; Low, J. J. H.; Ilancheran, A.; Huang, Z. Simultaneous Fingerprint and High-Wavenumber Confocal Raman Spectroscopy Enhances Early Detection of Cervical Precancer In Vivo. *Anal. Chem.* **2012**, *84* (14), 5913–5919.
- (58) Popp, J.; Brehm, B. R.; Romeike, B. F.; Egodage, K. D.; Dochow, S.; Matthäus, C. Detection and characterization of early plaque formations by Raman probe spectroscopy and optical coherence tomography: an in vivo study on a rabbit model. *Journal of Biomedical Optics* **2018**, *23* (01), 015004.
- (59) Noonan, J.; Asiala, S. M.; Grassia, G.; MacRitchie, N.; Gracie, K.; Carson, J.; Moores, M.; Girolami, M.; Bradshaw, A. C.; Guzik, T. J.; Meehan, G. R.; Scales, H. E.; Brewer, J. M.; McInnes, I. B.; Sattar, N.; Faulds, K.; Garside, P.; Graham, D.; Maffia, P. In vivo multiplex molecular imaging of vascular inflammation using surface-enhanced Raman spectroscopy. *Theranostics* **2018**, *8* (22), 6195–6209.
- (60) Römer, T. J.; Brennan, J. F.; Fitzmaurice, M.; Feldstein, M. L.; Deinum, G.; Myles, J. L.; Kramer, J. R.; Lees, R. S.; Feld, M. S. Histopathology of Human Coronary Atherosclerosis by Quantifying Its Chemical Composition With Raman Spectroscopy. *Circulation* **1998**, *97* (9), 878–885.
- (61) Buschman, H. P.; Motz, J. T.; Deinum, G.; Römer, T. J.; Fitzmaurice, M.; Kramer, J. R.; van der Laarse, A.; Bruschke, A. V.; Feld, M. S. Diagnosis of human coronary atherosclerosis by morphology-based Raman spectroscopy. *Cardiovascular pathology: the official journal of the Society for Cardiovascular Pathology* **2001**, *10* (2), 59–68.
- (62) Šćepanović, O. R.; Fitzmaurice, M.; Gardecki, J. A.; Angheloiu, G. O.; Awasthi, S.; Motz, J. T.; Kramer, J. R.; Dasari, R. R.; Feld, M. S. Detection of morphological markers of vulnerable atherosclerotic plaque using multimodal spectroscopy. *J. Biomed Opt* **2006**, *11* (2), No. 021007.
- (63) Silveira, L.; Sathaiyah, S.; Zângaro, R. A.; Pacheco, M. T. T.; Chavantes, M. C.; Pasqualucci, C. A. G. Correlation between near-infrared Raman spectroscopy and the histopathological analysis of atherosclerosis in human coronary arteries. *Lasers in Surgery and Medicine* **2002**, *30* (4), 290–297.
- (64) Nogueira, G. V.; Silveira, L.; Martin, A. A.; Zângaro, R. A.; Pacheco, M. T. T.; Chavantes, M. C.; Pasqualucci, C. A. Raman spectroscopy study of atherosclerosis in human carotid artery. *Journal of Biomedical Optics* **2005**, *10* (3), 031117.
- (65) Chau, A. H.; Motz, J. T.; Gardecki, J. A.; Waxman, S.; Bouma, B. E.; Tearney, G. J. Fingerprint and high-wavenumber Raman spectroscopy in a human-swine coronary xenograft in vivo. *J. Biomed Opt* **2008**, *13* (4), No. 040501.
- (66) Dochow, S.; Fatakdawala, H.; Phipps, J. E.; Ma, D.; Bocklitz, T.; Schmitt, M.; Bishop, J. W.; Margulies, K. B.; Marcu, L.; Popp, J. Comparing Raman and fluorescence lifetime spectroscopy from human atherosclerotic lesions using a bimodal probe. *Journal of Biophotonics* **2016**, *9* (9), 958–966.
- (67) Zhang, Y.; Chen, R.; Liu, F.; Miao, P.; Lin, L.; Ye, J. In Vivo Surface-Enhanced Transmission Raman Spectroscopy under Maximum Permissible Exposure: Toward Photosafe Detection of Deep-Seated Tumors. *Small Methods* **2023**, *7* (2), 2201334.
- (68) Bergholt, M. S.; Duraipandian, S.; Zheng, W.; Huang, Z. Multivariate reference technique for quantitative analysis of fiber-optic tissue Raman spectroscopy. *Anal. Chem.* **2013**, *85* (23), 11297–303.
- (69) Lussier, F.; Missirlis, D.; Spatz, J. P.; Masson, J. F. Machine-Learning-Driven Surface-Enhanced Raman Scattering Optophysiology Reveals Multiplexed Metabolite Gradients Near Cells. *ACS Nano* **2019**, *13* (2), 1403–1411.
- (70) Shu, C.; Yan, H.; Zheng, W.; Lin, K.; James, A.; Selvarajan, S.; Lim, C. M.; Huang, Z. Deep Learning-Guided Fiberoptic Raman Spectroscopy Enables Real-Time In Vivo Diagnosis and Assessment of Nasopharyngeal Carcinoma and Post-treatment Efficacy during Endoscopy. *Anal. Chem.* **2021**, *93* (31), 10898–10906.
- (71) Chen, X.; Shen, J.; Liu, C.; Shi, X.; Feng, W.; Sun, H.; Zhang, W.; Zhang, S.; Jiao, Y.; Chen, J.; Hao, K.; Gao, Q.; Li, Y.; Hong, W.; Wang, P.; Feng, L.; Yue, S. Applications of Data Characteristic AI-Assisted Raman Spectroscopy in Pathological Classification. *Anal. Chem.* **2024**, *96* (16), 6158–6169.
- (72) MacRitchie, N.; Frleta-Gilchrist, M.; Sugiyama, A.; Lawton, T.; McInnes, I. B.; Maffia, P. Molecular imaging of inflammation - Current and emerging technologies for diagnosis and treatment. *Pharmacology & Therapeutics* **2020**, DOI: 10.1016/j.pharmthera.2020.107550.